https://dx.doi.org/10.1016/j.conbuildmat.2020.120651

Simulation of the Field Aging of Asphalt Binders in Different Reclaimed Asphalt Pavement (RAP) Materials in Hong Kong through Laboratory Tests

Yu Qian[a], Feng Guo[b*], Zhen Leng[c*], Yuan Zhang[d], Huayang Yu[e]

[a]Assistant Professor, Department of Civil and Environmental Engineering, University of South Carolina, Columbia, SC, USA
[b]Graduate Research Assistant, Department of Civil and Environmental Engineering, University of South Carolina, Columbia, SC, USA. Former Research Assistant, Department of Civil and Environmental Engineering, The Hong Kong Polytechnic University, Hung Hom, Kowloon, Hong Kong Special Administrative Region, China
[c]Associate Professor, Department of Civil and Environmental Engineering, The Hong Kong Polytechnic University, Hung Hom, Kowloon, Hong Kong Special Administrative Region, China
[d]Research Associate, Department of Civil and Environmental Engineering, University of Wisconsin-Madison, Madison, WI, USA
[e]Associate Professor, Department of Civil and Environmental Engineering, South China University of Technology, Guangzhou, Guangdong, China
[*] Corresponding author

ABSTRACT: Nowadays, reclaimed asphalt pavement (RAP) are widely used in pavement construction because of its significant environmental and economic benefits. In general, the use of RAP can introduce significant reduction in emission generation, energy consumption, and construction cost. To better utilize RAP, previous studies have paid extensive efforts to accelerate and quantify aging of asphalt binders in the laboratory, with the hope to predict their long-term performance in the field. But unfortunately, the existing laboratory aging methods cannot fully represent the field conditions due to the complexity of the field aging environment, caused by various factors, such as the seasonal and local climate characteristics of the interested areas. This study aims to quantify the difference between the binder laboratory aging and field aging in subtropical climate, at Hong Kong. The chemical compositions, rheological properties, and engineering performance of the field-aged asphalt binders (FAB) from several local pavements were characterized and compared with those of the laboratory aged asphalt binders (LAB). Six FAB samples were obtained from the reclaimed asphalt pavement (RAP) mixtures which had served on urban roads at Hong Kong for different durations. In the laboratory, following the conventional approach, the rolling thin film oven test (RTFOT) followed by the (Pressure Aging Vessel (PAV) test were performed to

prepare the LAB samples. The results from the dynamic shear rheometer (DSR) and Fourier transform infrared spectrometer (FTIR) tests showed that the agings of the FAB samples were significantly higher than those of the LAB samples. Specifically, the conventional laboratory aging method for asphalt binder underestimated the field aging of a four-year old stone mastic asphalt (SMA) mixture nor a five-year old dense asphalt mixture. The results of this study suggested that more demanding aging process in the laboratory be developed for better simulation of the long-term field performance of asphalt mixture.

Key words: Field aging, MHS model, Reclaimed Asphalt Pavement, Pressure Aging Vessel

1. Introduction

Nowadays, there has been a great interest in the inclusion of recycled materials, such as reclaimed asphalt mixture (RAP), in pavement construction because of its significant environmental and economic benefits [1]. According to Cao et al. [2], with the service life of 15 years, hot in-place recycled pavement can save 5% cost and reduce 16% overall environmental impact by using eco-efficiency analysis (EEA), representing an eco-efficient solution for asphalt pavement rehabilitation. From the economic perspective, an increase of 10% RAP usage in warm stone mastic asphalt (SMA) material will result in lower construction cost compared with that of the control conventional hot SMA [3]. In addition, based on life cycle analysis, the combination of RAP and warm mix asphalt (WMA) can lead to the reduction of 12% CO_{2eq}, 15% energy and 15% water [4].

Typically, pavement would serve in the field for years under a variety of environmental factors, such as oxygen, UV rays, and moisture, before it gets reclaimed [5]. Thus, the binder in RAP is significantly aged which often leads to early fatigue and thermal cracking, and reduced life of pavement [6-8]. To better use RAP in the pavement, it is important to understand how the properties and performance of field aged asphalt binders (FAB) change over time. In other words, rapid, simple and accurate methods for simulating FAB are desired for the successful commercial exploitation of RAP [9]. To simulate field aging in the lab, numerous accelerated aging methods have been developed. Currently the popular accelerated aging methods to simulate short-term aging in the lab mainly include the thin film oven test (TFOT), modified thin film oven test (MTFOT), rotating flask test (RFT), rolling thin film oven test (RTFOT), and other similar tests [10]. In these tests, the asphalt binder was treated in a certain heating device with raised temperatures to simulate binder short-term aging associated with asphalt mixture preparation activities before traffic, for instance, mixing, transportation, laying, and compaction at high temperatures [11-13]. These tests usually provided satisfying short-term aging prediction, however, the high temperature treatment in these tests often causes high discrepancies in simulating the long-term aging of binders in the field [10].

To combat the inaccurate binder long-term aging predictions, many researchers have developed and modified laboratory testing procedures and facilities through combing thin film aging with oxidative aging. Lee [14] proposed an aging procedure for asphalt binders with 65 °C in a standard TFOT vessel with pure oxygen flow for 1,000 hours. It was concluded that after 46-hour aging, the asphalt binders can represent five-year field aging in Iowa, USA. Verhasselt [15, 16] developed the rotating cylinder aging test (RCAT) as an accelerated aging test. In this test, the temperature was controlled between 70 °C and 110 °C. An oxygen flow with a rate of 75 ml/min was introduced into the rotated cylinder with a rotation rate of 1 rpm. The conclusion was a test temperature below 100 °C can be used to simulate filed aging conditions. Besides, Choquet [17] conducted the RCAT at 85 °C for 144 hours. It was reported that the test under this condition can better simulate field aging in terms of the formation of asphaltenes in asphalt binders. It was also noted that the temperature under 100 °C was essential to simulate asphalt binder long-term field aging. The Strategic Highway Research Program (SHRP) developed a long-term aging simulation method by using Pressure Aging Vessel (PAV) [18] and it has been widely used across the world. This aging procedure requires to age asphalt binder in the RTFOT followed by oxidization in a pressurized aging vessel. To simplify the SHRP aging steps, Migliori and Corté [19] used an unmodified binder with a penetration grade of 35/50 to verify whether an extended PAV test can be used to replace the coupled RTFOT and PAV protocol. Based on their research outcome, it was concluded that: 1) there was an equivalence between 5h PAV and RTFOT at 100 °C and 2.1MPa; and 2) 25h PAV aging was equivalent to the aging of RTFOT plus 20h PAV. Verhasselt [15] compared the PAV aging and RCAT aging and found that 20h PAV aging was equivalent to 178h RCAT aging. Huang et al. [20] compared several artificial aging methods to simulate the field aging process. It was found that RTFOT at 185 °C appeared to be suitable to simulate one year of field aging of asphalt binder in the pavement mixture of AC-20 in Florida. In addition, the modified aging process with the California tilt oven was found to be suitable for simulating eight years of field aging. It is worth noting that all the findings mentioned above are associated with specific types of asphalt mixture samples and the local climate, which unfortunately cannot be easily extended to other mixtures or areas.

Hong Kong is one of the most populated metropolitan areas in the world, which has a typical humid sub-tropical climate and approximately 1,948 hours of sunshine per year [21]. A combination of relatively high pavement temperature, a large amount of rainfall, and high UV radiation level can cause severe aging of asphalt binders in the pavement. With a high volume of traffic, it is extremely difficult to arrange pavement rehabilitation activities considering the traffic demand in Hong Kong. Besides, the restrictions on landfill space, and environmental and political pressure have led the local Highways Department and academia to investigate potential approaches to maximizing the reuse of RAP in Hong Kong. To develop a guideline for the selection, design and construction of RAP mixture which can perform equivalently or better than the conventional virgin mixtures, it is important to characterize the aging of asphalt binders in the field and determine suitable laboratory aging methods which can reasonably simulate the field aging.

2. Research Objective and Scope

This study aims to address the urgent need of investigating the binder field aging characteristics and exploring appropriate laboratory testing protocols to simulate the binder field aging in Hong Kong. To achieve this objective, field-aged asphalt binders (FAB) were collected from the local roads and their engineering performance, rheological properties, and chemical compositions were tested. The testing results of aging levels of FAB samples were compared with the values obtained from the laboratory-aged asphalt binder (LAB) samples. Typical local asphalt mixtures with different service years were investigated.

3. Materials and Test Methods

3.1. Materials preparation

Six different RAP materials were collected from local roads at Hong Kong (see Fig. 1). Two types of asphalt mixtures popular in Hong Kong were included: gap-graded stone mastic asphalt (SMA) and dense-graded wearing course (WC). Ideally, the thickness of RAP layer should be considered to make fair comparisons. It is worth noting that in Hong Kong, the typical thickness for both WC and SMA mixtures

are 40mm no matter whether the pavement is for urban roads or expressways. The maximum aggregate sizes of those paved SMA and WC varied between 10mm and 20mm. The FAB samples were extract from the collected RAP. Each FAB sample was named based on the original mixture design and its age. For example, FAB sample "SMA4" was obtained from an SMA mixture which had been used in the field for four years by the time when it was reclaimed. In addition to the FABs, the virgin asphalt binder used for those local roads, which is from a local supplier and has a penetration grade of 60/70 (Pen 60/70), was obtained and aged in the laboratory for comparison purpose. Each LAB sample was named based on the number of laboratory aging cycles it went through. For example, sample "LAB1" means the virgin binder went through one cycle of 20h aging in the laboratory. Details of all tested samples are provided in Table 1.

Fig. 1. Sampling sites at Hong Kong shown in Google Map

Table 1. Information of tested FAB and LAB materials

Sample	Type of asphalt mixture/Binder	Location of pavements	Service time (year)	PAV aging time (h)
Pen60/70	-	-	-	--
SMA4	SMA	Queensway West Bound	4	
SMA9		Ho Pui Street	9	-
SMA12		Cannaught Road Central	12	-
WC5	WC	Cheung Tat Road	5	-
WC19		Route Twisk	19	-
WC27		Po Fung Road	27	-
LAB1	-	-	-	20
LAB2	-	-		40
LAB3	-	-	-	60

The FAB samples were extracted from the RAP materials following in accordance with ASTM D2172 [22] and ASTM D5405[23]. Dichloromethane (DCM) was used as the solvent for extraction. Centrifugation at 2,500 rpm for 30 mins was first conducted to remove the filler particles from the asphalt-solvent solution. Then, the rotatory evaporation at 80 °C for 2h was applied to remove the solvent from the solution. It has been confirmed that this recovery procedure would not cause any additional aging based on the measuring results from Fourier transform infrared spectroscopy (FTIR) test which is a simple but effective technique and has been widely used to characterize the changes of chemical functional groups of asphalt binder [24-30]. Besides, it was found that the solvent could be thoroughly removed from the binder since there was no interference in following spectra results [31-34]. Fig. 2 shows the detailed steps for RAP binder extraction.

Fig. 2. Procedure to recover RAP binder

The LAB samples were prepared from virgin Pen 60/70 asphalt binder through RTFOT followed by PAV test according to AASHTO 240 [35] and AASHTO R 28 [18], respectively. In addition, the PAV aging time was extended to 40h and 60h, aiming to simulate more extensive aging in the laboratory which might be more representative of the field aging. Fig. 3 shows the procedures in the lab to prepare LAB samples through RTFOT and PAV.

Fig. 3. Procedure to prepare LAB samples

3.2. Test methods

The conventional engineering properties, including softening point and penetration, of the binders were measured in accordance with ASTM D36 [36] and ASTM D5 [37], respectively. The high-temperature behaviors of virgin and aged binder samples were characterized by Superpave rutting factor according to

AASHTO M320 [38]. The initial test temperature was 64 °C and then an increasing interval of 6 °C was employed. A strain level of 12% was applied at each testing temperature until the measured rutting factor was lower than 1.0 kPa (for the virgin binder) or 2.2 kPa (for the LAB and FAB).

The dynamic shear rheometer (DSR), model MCR702 manufactured by Anton Paar, was used to perform frequency sweep test according to AASHTO T315 [39]. The 8mm-diameter parallel plates were used at the temperatures ranging from 4 °C to 40 °C, with an interval of 12 °C, and the gap between top and bottom parallel plates was 2mm. Besides, the 25mm-diameter parallel plates were used at 52 °C to 76 °C with an interval of 12 °C, and the gap was 1mm. Before running the test at each test temperature, the samples were kept warm at the air chamber for 600s. During the tests, the frequency was set ranging from 0.1 to 30 Hz. Notably, the frequency sweep test of each FAB sample was performed within the linear viscoelastic region (LVE) and the strain level ranged from 0.05% to 5. Lastly, the data were collected and processed to construct the master curve which was useful to predict viscoelastic properties over a wide frequency and temperature range.

In addition, FTIR tests were conducted on all binder samples. Approximately 1 g of binder sample was fixed on the reflection diamond accessory for the FTIR tests. The wavenumbers were set at a range of 4000 cm^{-1} to 600 cm^{-1} and the resolution was 4 cm^{-1}. It is worth noting that FTIR test results were sensitive to the thickness of the sample [29]. To avoid the thickness interference, spectral normalization was applied in the full infrared spectrum range using the OMNIC software.

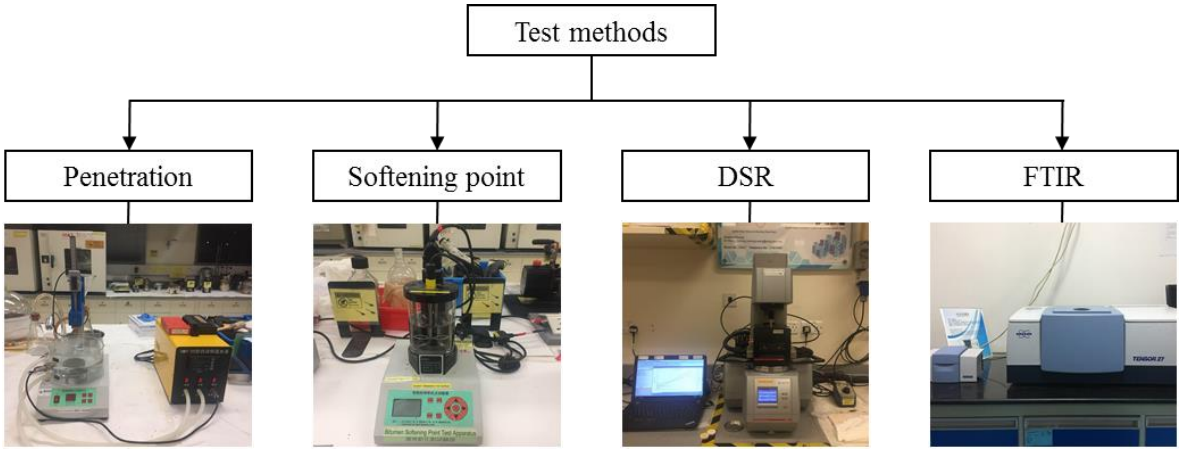

Fig. 4. Test methods and equipment performed in this paper

4. Results and Discussions

4.1. Penetration and softening point

Typically, PAV is expected to simulate 5 to 10 years of in-service aging of asphalt binder. To make fair comparisons, ideally, the traffic and environmental conditions should be consistent for all the site. However, it is not feasible to strictly control the field conditions. It should be noted that the field samples may still experience quite different traffic and environmental conditions even they were collected from the same city. In this study, each test was repeated three times. LAB1 sample was used to simulate the approximate 5 years old FAB sample, LAB2 sample was used to simulate the approximate 10 years old FAB sample, and LAB3 sample was used to investigate the aging effect of FAB sample with much longer time.

Fig. 5 shows the softening point and penetration values of all the asphalt binders tested in this study. The error bars showing in Fig.5 are with a 95% confidence interval. It can be observed that the penetration values decreased while the softening point values increased, with the extension of the aging time, which is as expected. WC27 sample has the maximum value of softening point, 79 °C, and the minimum value of penetration, 0.6mm, indicating it is the most aged sample among all the tested materials.

The values of the penetration and softening point of LAB1 are 1.7mm and 63.1 °C, respectively. Since PAV aging is expected to simulate 5 to 10 years in-service aging of asphalt binders, the penetration and softening point of LAB1 were compared with the values of SMA4 and WC5. Based on Fig. 5, SMA4 has a softening point at 58.9 °C which is lower than the value of LAB, however, the penetration value of SMA4 is 2.2mm, higher than the value of LAB1, suggesting SMA4 and LAB1 have different aging levels. Besides the comparison between SMA4 and LAB1, the penetration and softening point for WC5 are 1.9mm and 62.2 °C, respectively, which are 0.2mm higher and 0.9 °C lower than the value of LAB1. The comparison between WC5 and LAB1 also shows the aging levels of LAB1 and WC5 are not the same. Thus, the standard PAV procedure did not achieve the same aging level that the field aged asphalt binder gained after 4 or 5 years' service in terms of their penetration and softening point values.

To exam whether the extended 40h PAV aging could simulate approximately 10 years field aging, the penetration and softening point values of LAB2 and SMA9 are compared. Specifically, the penetration value of SMA9 is 1.55 mm which is close to 1.4mm-penetration of LAB2, whereas the softening point of LAB2, 67.0 °C, is 4.5 °C higher than the softening point at 62.5 °C of SMA9, indicating LAB2 and SMA9 had different aging levels.

To investigate the effect of 60h PAV aging, the values of softening point and penetration of LAB3 are compared with the rest FAB samples. Compared with WC27, LAB 3 had a lower softening point of 69.9 °C, and a higher penetration value of 1.3mm, indicating 60h lab PAV aging has not reached the same aging level of WC27. It was also noted that the softening point value of LAB3 is similar to that of SMA12 (70.3 °C), but the penetration value of SMA12 (0.94mm) is lower than that of LAB3. Lastly, by comparing WC19 and LAB3, no similar values of penetration and softening point were observed. The softening point and penetration tests are typically used for quick aging assessment, which may not fully reflect the actual aging conditions of the binders. Thus, more tests are conducted to better evaluate the sample aging levels, such as DSR and FTIR tests.

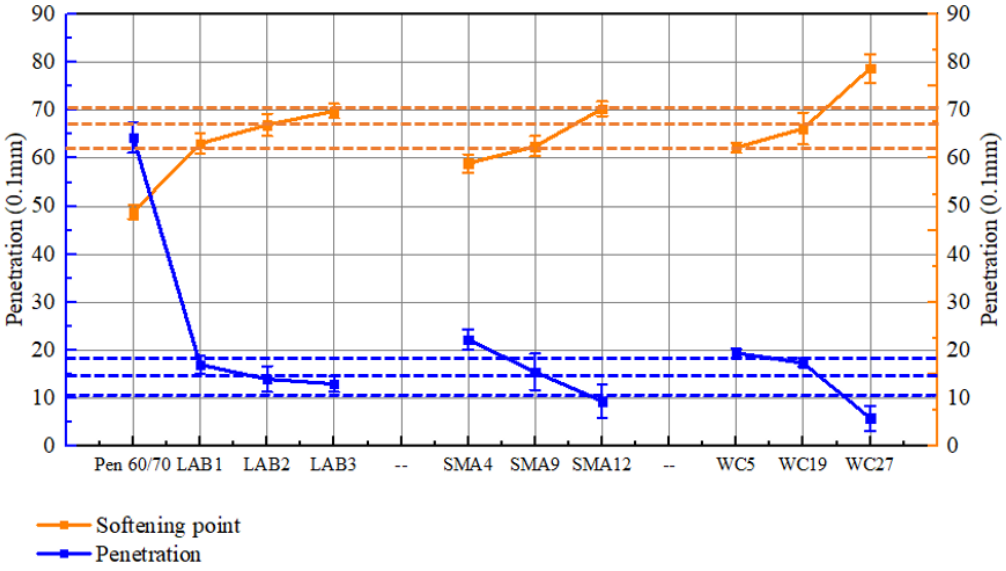

Fig. 5 Test results of softening point & penetration for asphalt binder samples

4.2. Rutting parameter

Fig. 6 presents test results of the Superpave rutting parameter ($G^*/\sin\delta$), which is often used to indicate the performance of asphalt binders at a high temperature. It is clear that with the increasing of temperature, the rutting parameter decreases for each sample. The rutting parameter value at 64℃ was selected as an aging indicator to compare the aging levels of different samples since it is the highest value in each test for each sample before sample failure. As shown in the Fig. 6(a), SMA12 and WC27 have the highest rutting parameters which are 364.44 kPa and 364.48 kPa, respectively. Obviously, SMA12 and WC27 have much larger rutting parameters than the others, largely due to their relatively longer service periods, 12 years and 27 years in the field. Fig. 6(b) and (c) show more details of Fig. 6(a). Fig. 6(b) shows the rest samples with relatively low rutting parameter values, while Fig. 6(c) presents a close comparison of SMA12 and WC27 which have relatively high rutting parameter values. Based on the highest value of each curve in Fig. 6(a), the aging ranking can be sorted as shown in Table 2.

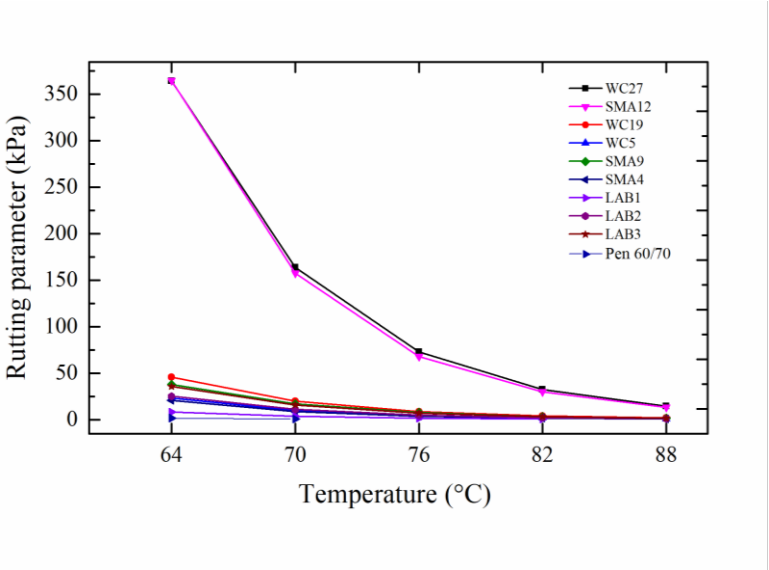

230

231 (a)

232

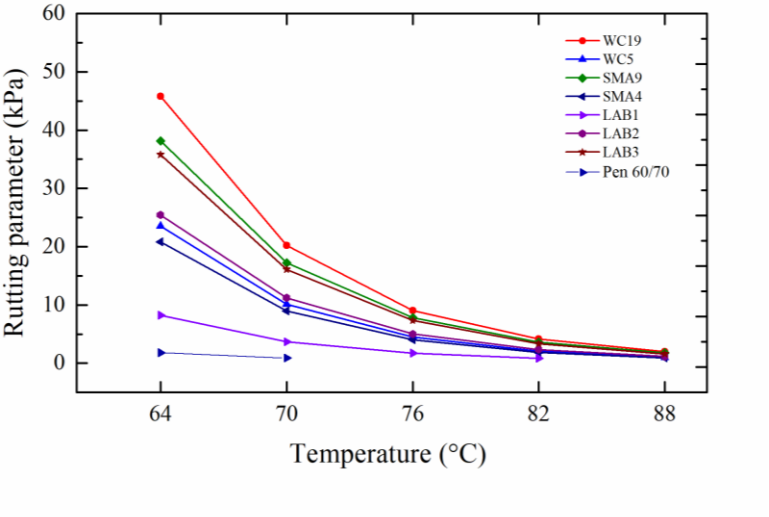

233

234 (b)

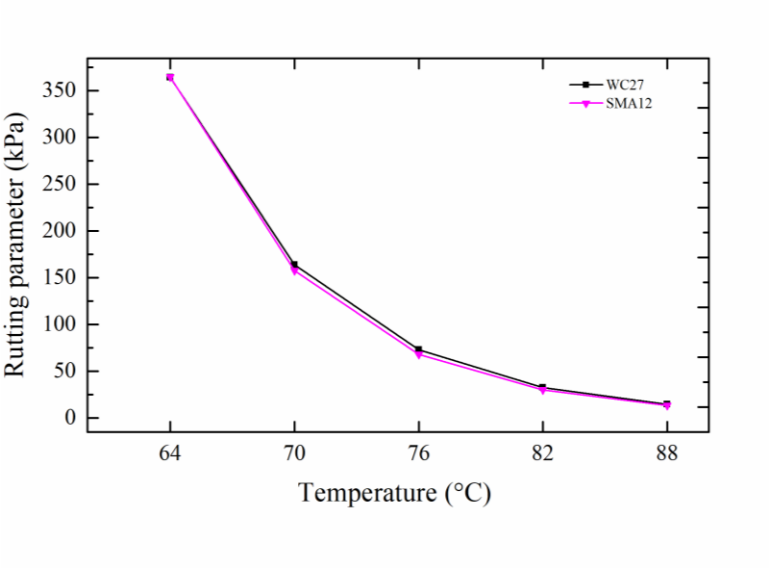

(c)

Fig. 6. Rutting parameter of the asphalt binder samples

Table 2. Ranking of highest rutting parameter values of tested samples

Sample ID	Rutting parameter (kPa)	Ranking
WC27	364.48	1
SMA12	364.44	2
WC19	45.81	3
SMA9	38.14	4
LAB3	35.79	5
LAB2	25.42	6
WC5	23.51	7
SMA4	20.84	8
LAB1	8.23	9
Pen60/70	1.81	10

From Table 2, we can see the rutting parameter of LAB1 is 8.23kPa, which is lower than that of SMA4, 20.84 kPa. This discrepancy, which is consistent with the differences in penetration and softening point presented earlier, again indicates the standard PAV aging cannot represent four years of filed aging of SMA binders in Hong Kong. On the other hand, the rutting parameters of LAB2, WC5 and SMA4 are 25.42 kPa, 23.51kPa, and 20.84kPa, respectively, which are close to each other. The rutting parameters of LAB3 and SMA9 are 35.79kPa and 38.14kPa, respectively, which are also similar. Thus, the lab aging

condition for LAB3 and LAB2 could potentially be used to represent the filed aging condition for SMA9 and WC5/SMA4 in Hong Kong, respectively, in term of the rutting parameter.

4.3. Master curve

The rheological properties of LAB and FAB under a variety of frequency and temperature conditions were evaluated using the master curves which had been successfully applied in the previous studies to characterize asphalt binders [27, 40-43]. The master curves in this study were constructed at a reference temperature of 25 °C [40]. The shift factors used to shift the data points tested at different temperatures to the reference temperature were determined by the Williams-Landel-Ferry (WLF) formula shown in Equation (1).

$$\log a_T = \frac{-C_1(T-T_0)}{C_2+(T-T_0)} \quad (1)$$

where a_T is the shift factor; C_1 and C_2 are constants; T_0 is the selected reference temperature; T is the test temperature.

After the master curves were constructed, they were fitted with the Modified Huet-Sayegh (MHS) model which was developed by Woldekidan et al. [44]. Compared with the Huet-Sayegh (HS) model [45] and the Christensen-Anderson (CA) model [46, 47] which are commonly adopted in the rheological characterization of asphalt binders, the MHS model improves data fitting in the low frequency region. Meanwhile, because there is an additional linear dashpot (compared with the HS model), MHS model can also be used to simulate the viscous deformation. The MHS model can be explained by Equations (2-8)

$$J^*(\omega) = \frac{G'}{|G^*(\omega)|^2} - i\left[\frac{G''}{|G^*(\omega)|^2} + \frac{1}{\eta_3\omega}\right] = J'(\omega) - iJ''(\omega) \quad (2)$$

where G^* is the complex shear modulus in the HS model; G' is the storage shear modulus in the HS model; G'' is the loss shear modulus in the HS modulus; η_3 is linear dashpot parameter; $J^*(\omega)$ is the

complex creep compliance in the MHS model; $J'(\omega)$ is the storage creep compliance in the MHS model; and $J''(\omega)$ is the loss creep compliance in the MHS model.

$$G^*(\omega) = G_0 + \frac{G_\infty - G_0}{1+\delta_1(i\omega\tau_1)^{-m_1}+\delta_2(i\omega\tau_2)^{-m_2}} \quad (3)$$

$$\delta_i = \frac{\tau_{1(G_\infty - G_0)}}{\eta_i} \quad (4)$$

$$G' = G_0 + A\frac{G_\infty - G_0}{A^2+B^2} \quad (5)$$

$$G'' = B\frac{G_\infty - G_0}{A^2+B^2} \quad (6)$$

$$A = 1 + \delta_1\frac{\cos(m_1\frac{\pi}{2})}{(\omega\tau)^{m_1}} + \delta_2\frac{\cos(m_2\frac{\pi}{2})}{(\omega\tau)^{m_2}} \quad (7)$$

$$B = 1 + \delta_1\frac{sin(m_1\frac{\pi}{2})}{(\omega\tau)^{m_1}} + \delta_2\frac{sin(m_2\frac{\pi}{2})}{(\omega\tau)^{m_2}} \quad (8)$$

where G_∞ is the instantaneous shear modulus; G_0 is the rubbery shear modulus; δ_1 and δ_2 are model parameters; m_1 and m_2 are the parabolic dashpot coefficients; η_1 and η_2 are parabolic dashpots' parameters; τ_1 and τ_2 are the time constants; and A and B are the variables.

Based on a previous study [27], seven parameters are needed in the MHS model to describe the complete responses of FAB and LAB in different temperature and frequency ranges, which are m_1, m_2, δ_1, τ, G_∞, G_0, and η_3, respectively. Table 3 shows the calculated model parameters of the master curves from the samples in this study. The constructed master curves of all LAB and FAB samples are presented in Fig. 7 to Fig. 9.

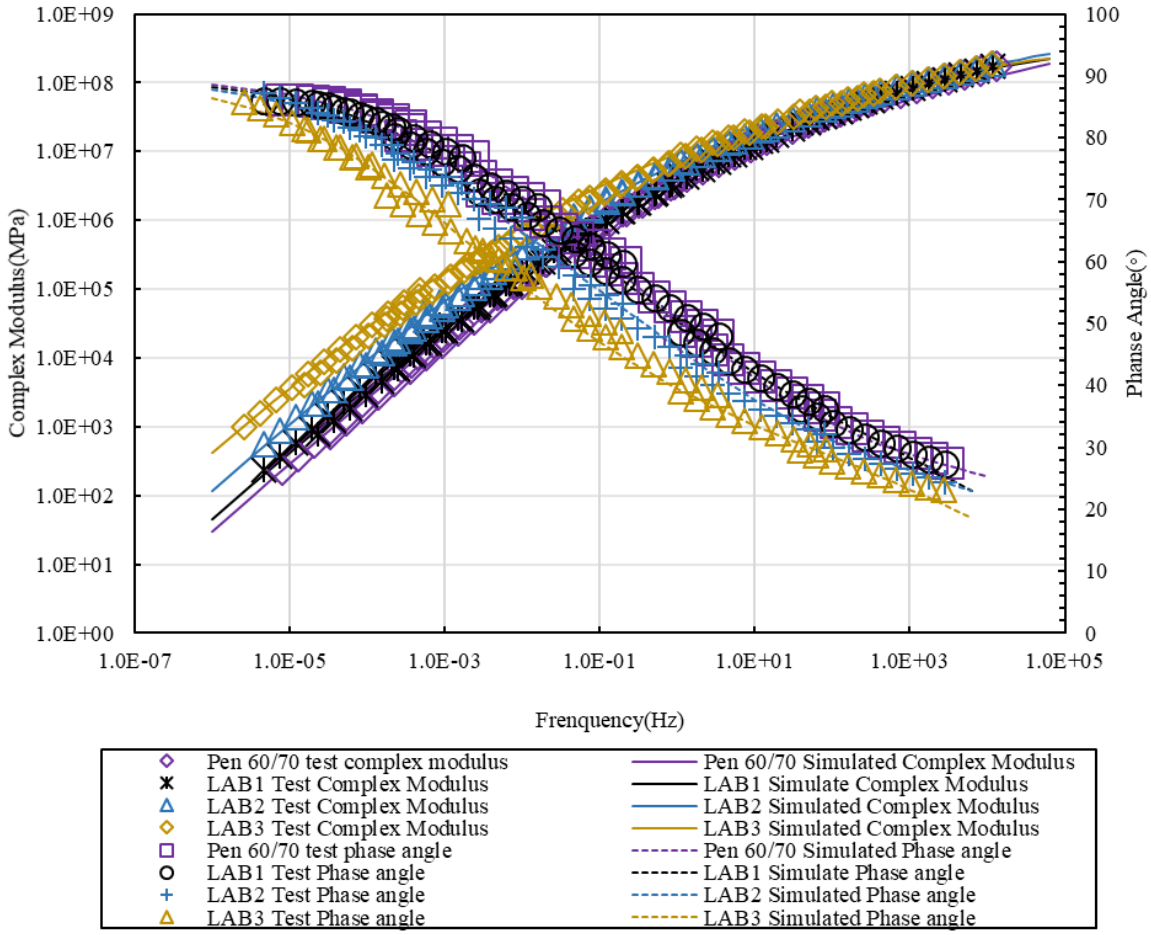

284

285 **Fig. 7 The master curves of fresh binder and LAB samples**

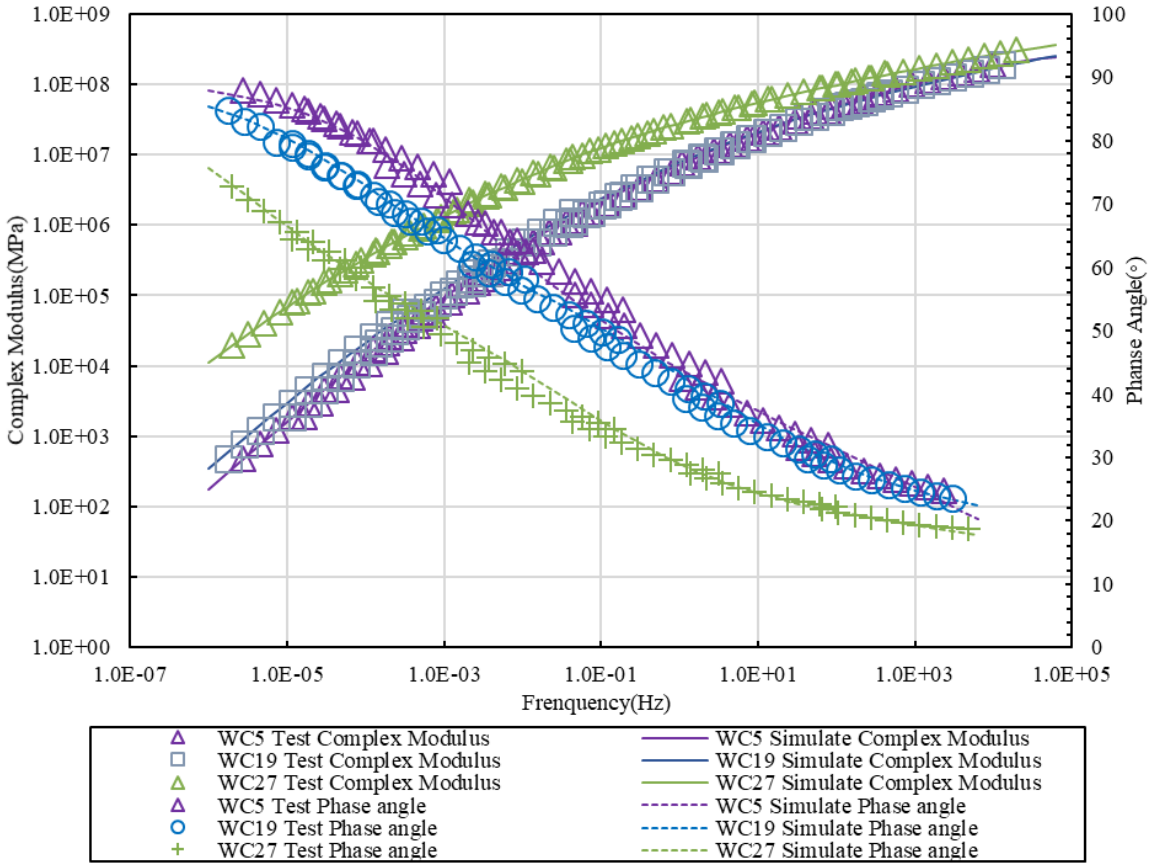

286

287 **Fig. 8 The master curves of FAB samples recovered from WC**

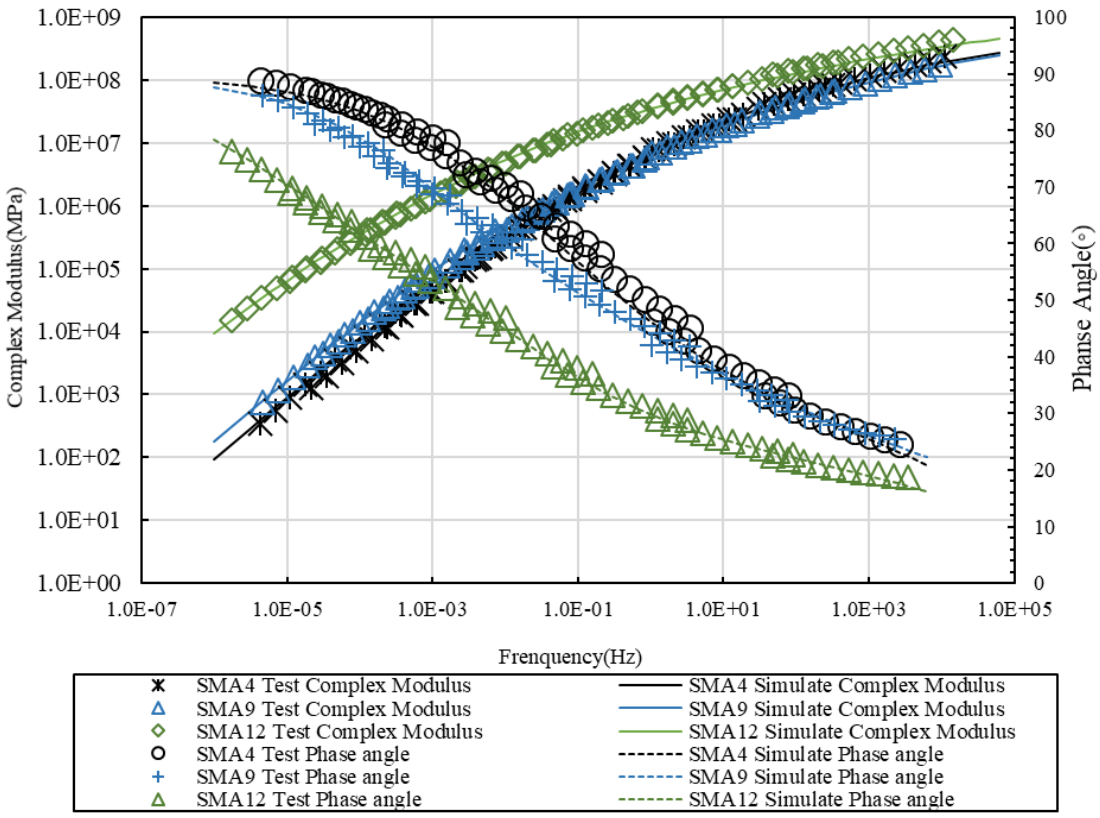

Fig. 9 The master curves of FAB samples recovered from SMA

Table 3. The parameters of MHS model for tested materials

Sample	C_1	C_2	m_1	m_2	δ_1	τ	G_∞	G_0	η_3	R^2	
										G^*	δ
SMA4	24.363	220.410	0.654	0.322	2.48E-02	2.70E-06	5.25E+08	2.04E-01	1.57E+07	0.9992	0.9964
SMA9	25.373	234.212	0.291	0.608	6.07E+00	1.98E-04	6.77E+08	5.03E-02	3.07E+07	0.9996	0.9958
SMA12	29.569	252.98	0.270	0.633	9.82E+00	1.19E-02	8.80E+08	1.00E+00	2.25E+09	0.9990	0.9974
WC5	30.450	274.097	0.621	0.315	4.81E-02	3.35E-06	4.67E+08	2.23E-01	2.53E+07	0.9993	0.9956
WC19	31.697	274.660	0.659	0.289	2.56E-03	6.25E-06	7.21E+08	5.07E-03	8.50E+09	0.9994	0.9918
WC27	34.269	298.928	0.238	0.032	1.02E+01	3.21E-03	1.13E+09	4.31E-02	3.70E+09	0.9991	0.9969
Pen 60/70	15.12	138.46	0.311	0.622	5.46E+00	1.46E-05	1093.37	2.03E-02	0.71	0.9998	0.9970
LAB1	22.871	206.297	0.670	0.347	3.67E-02	3.08E-06	4.25E+08	2.02E-01	7.96E+06	0.9993	0.9966
LAB2	24.746	220.074	0.321	0.657	7.19E+00	5.16E-04	5.50E+08	5.03E-02	2.48E+07	0.9998	0.9973
LAB3	28.533	253.079	0.290	0.605	6.79E+00	4.14E-04	6.31E+08	2.04E-01	6.82E+07	0.9997	0.9960

Fig. 7 to Fig. 9 show good fitting of the data with the MHS models, which is also confirmed by the high coefficient of determination (R^2) of G^* and δ presented in Table 3 (all above 0.99). It is obvious that the differences between the master curves in in Fig. 7 are smaller than those in Fig. 8 and Fig. 9, indicating the aging levels of the LAB samples are not so significant as the FAB samples. In high frequency region, LAB3 sample has the highest complex shear modulus and lowest phase angle among all LABs, confirming LAB3 sample is the most aged in Fig. 7. In Fig. 8, the most aged sample is WC27, while SMA12 is the most aged sample in Fig. 9.

To compare the aging level for all tested materials by using the parameters provided in the MHS model, G_∞ is selected as the indicator since G_∞ is the parameter that can determine the peak of master curves obtained from the MHS model. In addition, G_∞ is directly related with the ultimate complex modulus that can well represent the stiffness of the tested samples. Fig. 10 provides the G_∞ values of different tested materials sorted based on the magnitudes, which shows the following ranking from high to low: WC27 > SMA12 > WC19 > SMA9 > LAB3 > LAB2 > SMA4 > WC5 > LAB1 > Pen60/70, which is mostly consistent with the ranking according to Table 2, except for SMA4 and WC5. Table 2 shows WC5 > SMA4. According to Fig. 10, WC5 is more aged than LAB1, and SMA9 is more aged than LAB3, indicating more demanding aging process is required in the laboratory for better prediction of the long-term field aging under Hong Kong's climate condition.

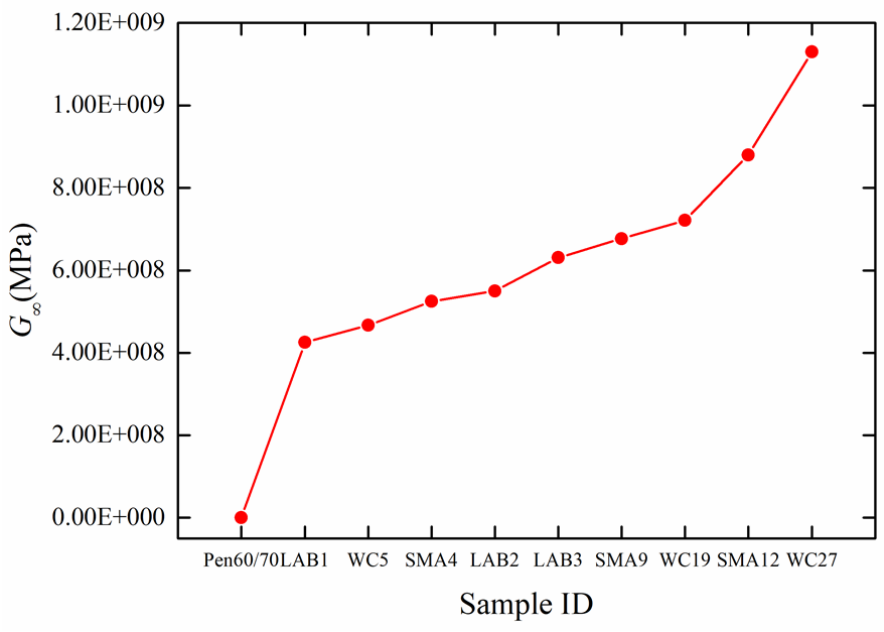

311

312 **Fig. 10. The instantaneous shear modulus (G_∞) of the tested materials**

313

314 4.4. FTIR test

315 The FTIR tests were performed to compare the changes of functional groups of the asphalt binder samples
316 before and after different aging conditions. The detailed information of the specific bands investigated
317 within FTIR spectrum were categorized as shown in Table 4 [30, 48, 49]. According to the previous
318 studies [25-27, 29, 30], the carbonyl group (C=O) at 1,700 cm^{-1} and the sulfoxide group (S=O) at 1,030
319 cm^{-1} were sensitive to the oxidation process. Accordingly, the carbonyl index (Ci) and the sulfoxide index
320 (Si) calculated from band areas with Equations (4) and (5) can be used as an indicator of asphalt binder
321 aging levels. In addition, the total index (Ti) of Ci and Si [50] was also calculated as a new aging index to
322 minimize the influence of the undocumented binder sources.

323 $$\text{Carbonyl Index} = \frac{A_{1700}}{\sum A} \quad (9)$$

324 $$\text{Sulfoxide Index} = \frac{A_{1030}}{\sum A} \quad (10)$$

Total Index= Carbonyl index + Sulfoxide index

where A_{1700} and A_{1030} are the areas of carbonyl and sulfoxide band, at 1700 cm^{-1} and 1030 cm^{-1}, respectively. $\sum A$ is $A_{1700}+A_{1600}+A_{1460}+A_{1376}+A_{1030}+A_{864}+A_{814}+A_{743}+A_{724}$, the sum areas of specific band between 2000 cm^{-1} and 600 cm^{-1}.

Table 4. Assignations of the main bands of the FTIR spectra

Wavenumber (cm^{-1})	Assignations
3594,3735	Stretching O–H
2924,2853	Stretching C–H aliphatic
1735	Stretching C=O
1700	Stretching C=O conjugated
1600	Stretching C=O aromatic
1460	Bending C–H of $–(CH_2)_n–$ (aliphatic index)
1376	Bending C–H of CH_3 (aliphatic branched)
1030	Stretching S=O sulfoxide
966	Bending C–H trans disubstituted –CH= CH– (butadiene block)
748,690	Bending C–H aromatic monosubstituted (styrene block)

Fig. 11 shows a representative FTIR test result of asphalt binder recovered from WC based RAP material. There are obvious changes in the carbonyl group and the sulfoxide group for different filed aging time periods. WC27 has the highest peaks and biggest areas of oxidative groups and WC5 has the lowest peaks and smallest areas of oxidative groups, indicating WC27 is the most aged sample in Fig. 11. To compare the aging levels of different samples, the oxidative indices, including Ci, Si, and Ti, are summarized in Table 5 and Ti is plotted in Fig. 12.

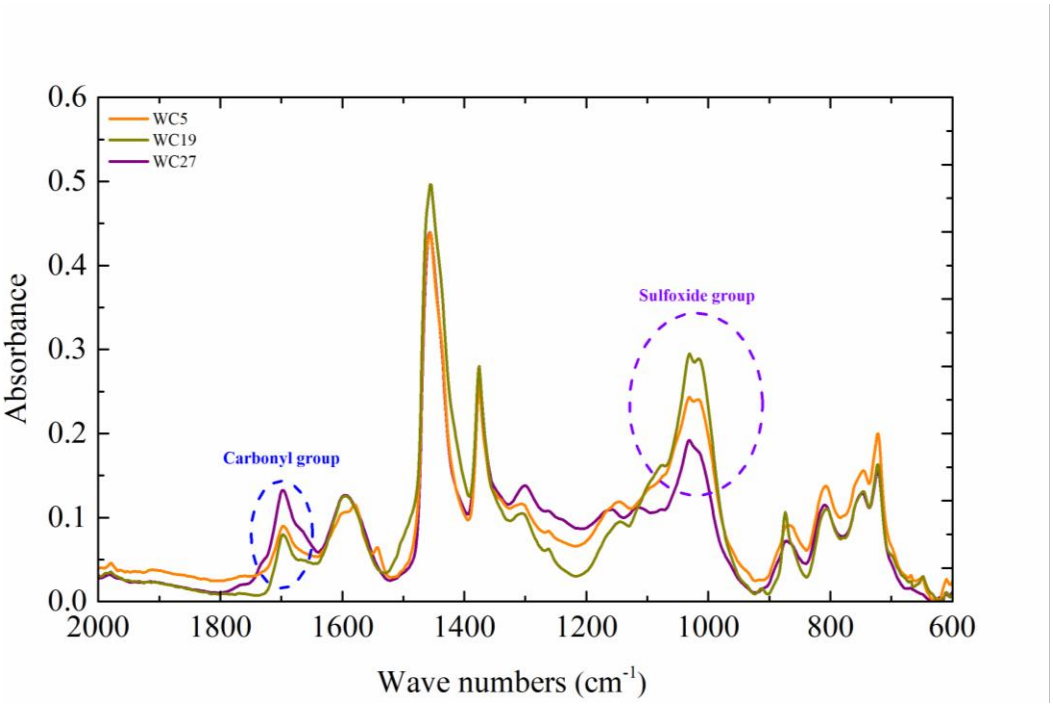

Fig. 11. Representative FTIR test results

Table 5. Oxidative indexes

Sample	Service year (s)	Aging hour (s)	Ci	Si	Ti
SMA4	4		0.029	0.075	0.104
SMA9	9		0.041	0.064	0.105
SMA12	12		0.046	0.081	0.127
WC5	5		0.045	0.077	0.122
WC19	19		0.030	0.095	0.125
WC27	27		0.098	0.070	0.168
Pen60/70	-	0	0	0.030	0.030
LAB1	-	20	0.0089	0.048	0.057
LAB2	-	40	0.033	0.046	0.079
LAB3	-	60	0.056	0.048	0.104

Table 5 presents the Ci and Si values of all binder samples. For SMA based field aged sample, the Ci values have an increasing trend when the service year increases but there is no similar trend in Si values. For example, the Ci value of SMA9, 0.041, is greater than the Ci value of SMA4, 0.029, showing an increasing trend. However, the Si values of SMA4 and SMA9 are 0.075and 0.064, respectively. For aged samples extracted from WC mixtures, there is no obvious correlation between Ci or Si values and the

service year. In summary, for LABs, Ci values increase with the extend of PAV aging time, but Si value was not sensitive to the PAV aging time.

To further explore the relationship between the oxidative index and aging levels of the tested samples, Ti was compared in Fig. 12. Referring to the data in Table 5, for FABs from WC mixtures, an increasing trend of Ti with the extension of the field aging time can be observed. For example, the values of Ti for WC5, WC19, and WC27 are 0.122, 0.125, and 0.168, respectively. Similar trend can be identified for FABs from SMA mixtures and the LABs with different PAV aging times. Hence, for the binder samples investigated in this study, it is reasonable to use Ti as an indicator to predict asphalt binder's aging degree rather than just to use Si or Ci alone.

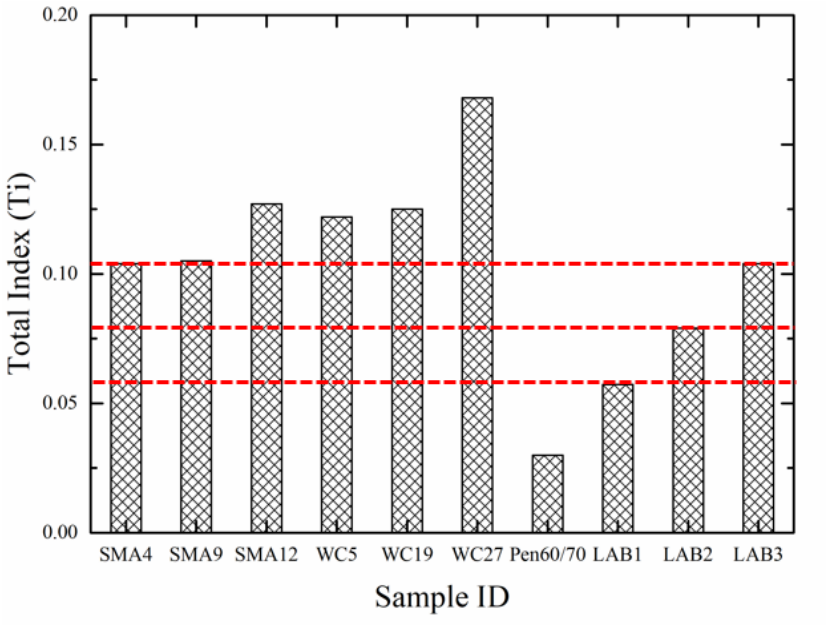

Fig. 12. Total index of experimental samples

In Fig. 12, WC27 has the largest value indicating its highest aging level. Meanwhile, LAB1 has much lower value of Ti than SMA4 and WC5, indicating that traditional PAV aging underestimates the 4- or 5-year field aging effect under Hong Kong's climate condition. It can also be observed that Ti value of LAB3 is close to the values of SMA4 and SMA9, suggesting similar aging levels.

To compare the aging levels based on different approaches, the results in Table 2, Fig. 10 and Fig. 12 were summarized into Table 6. In Table 6, it is clear that the rankings of the top 3 aged materials are fixed. In other words, the most aged three samples are WC27, SMA12 and WC19, regardless of the evaluation approach. In addition, WC5 and SMA4 were characterized as more aged than LAB3 and LAB2 when the chemical approach was used. The results in Table 2 and Fig. 10 indicated that LAB3 is much more aged than SMA4. However, in Table 6, they have the same Ti, indicating similar aging level. Thus, more research should be conducted in future studies on the potential correlations between the chemical approach and rheological approach for determine the aging levels of asphalt binders.

Table 6. Ranking of asphalt binder aging level with different approaches (smaller number indicates higher aging)

Sample ID	Ranking based on chemical approach (Ti value)	Ranking based on rheological approach (Rutting parameter)	Ranking based on rheological approach (G_∞)
WC27	1	1	1
SMA12	2	2	2
WC19	3	3	3
SMA9	5	4	4
LAB3	6	5	5
LAB2	8	6	6
SMA4	6	8	7
WC5	4	7	8
LAB1	9	9	9
Pen60/70	10	10	10

5. Summary and Findings

This study quantified the difference between the binder with laboratory aging and field aging under Hong Kong's climate condition. The chemical compositions, rheological properties, and engineering performance of the FAB samples were characterized and compared with those of the LAB samples. The following points summarize the major findings of this study:

- The field aged binders recovered from WC and SMA mixtures become harder as the mixture service time increases, as evidenced by the increased softening point values and decreased penetration values.

- Pen 60/70 binder after three PAV aging cycles has similar rheological properties with SMA9 and WC19, while Pen 60/70 after two PAV aging cycles has similar rheological properties with WC5 and SMA4.

- The field aged binders recovered from WC 27 and SMA12 are most aged based on rheological and FTIR test results. Even three PAV aging cycles is not enough to simulate the long-term field aging effect on binders in Hong Kong.

- Comparison between the rheological and chemical properties of Pen 60/70 after one PAV aging cycle and those of SMA4 indicated that one normal PAV aging cycle cannot simulate 4-year field aging effect under Hong Kong's climate condition.

Overall, the conventional PAV method was found to underestimate the long-term field aging of asphalt binder under Hong Kong's climate condition and most likely in other regions with similar climate condition. More demanding aging process in the laboratory should be developed for better simulation of the long-term field aging of asphalt binder in asphalt pavement.

6. Acknowledgement

The authors would like to thank the Hong Kong Research Grant Council for the financial support for the study presented in this paper (Project Number: 15214615).

References

[1] I.L. Al-Qadi, M. Elseifi, S.H. Carpenter, Reclaimed asphalt pavement—a literature review, 2007.
[2] R. Cao, Z. Leng, M.S.-C. Hsu, Comparative eco-efficiency analysis on asphalt pavement rehabilitation alternatives: Hot in-place recycling and milling-and-filling. Journal of cleaner production 210 (2019): 1385-1395.

[3] Z. Leng, I. Al-Qadi, Comparative life cycle assessment between warm SMA and conventional SMA, 2011.
[4] M.I. Giani, G. Dotelli, N. Brandini, L.J.R. Zampori, Conservation, Recycling, Comparative life cycle assessment of asphalt pavements using reclaimed asphalt, warm mix technology and cold in-place recycling, 104 (2015) 224-238.
[5] G. Xu, H. Wang, W.J.C. Sun, B. Materials, Molecular dynamics study of rejuvenator effect on RAP binder: Diffusion behavior and molecular structure, 158 (2018) 1046-1054.
[6] B.F. Bowers, B. Huang, X. Shu, B.C. Miller, Investigation of Reclaimed Asphalt Pavement blending efficiency through GPC and FTIR, Construction and Building Materials 50(Supplement C) (2014) 517-523.
[7] X. Lu, U. Isacsson, Effect of ageing on bitumen chemistry and rheology, Construction and Building Materials 16(1) (2002) 15-22.
[8] Z.-G. Feng, J.-Y. Yu, H.-L. Zhang, D.-L. Kuang, L.-H. Xue, Effect of ultraviolet aging on rheology, chemistry and morphology of ultraviolet absorber modified bitumen, Materials and Structures 46(7) (2013) 1123-1132.
[9] H.F. Haghshenas, Asphalt Binder Laboratory Short-Term Aging, (2019).
[10] G.D. Airey, State of the Art Report on Ageing Test Methods for Bituminous Pavement Materials, International Journal of Pavement Engineering 4(3) (2003) 165-176.
[11] EN 12607–1 Bitumen and bituminous binders–Determination of the resistance to hardening under the influence of heat and air–Part 1: RTFOT method, European Committee for Standardization, 2014.
[12] EN 12607–2 Bitumen and bituminous binders–Determination of the resistance to hardening under the influence of heat and air–Part 2: TFOT method, European Committee for Standardization, 2014.
[13] EN 12607–3 Bitumen and bituminous binders–Determination of the resistance to hardening under the influence of heat and air–Part 3: RFT method, European Committee for Standardization, 2014.
[14] D.-Y. Lee, Asphalt durability correlation in Iowa, 1973.
[15] V. AF, A kinetic approach to the aging of bitumens, Developments in petroleum science 40 (2000) 475-497.
[16] A. Verhasselt, F. Choquet, A new approach to studying the kinetics of bitumen aging, Proc of Int Symp on Chemistry of Bitumen, 1991, pp. 686-705.
[17] F. Choquet, Bitumen Ageing, Centre de Recherces Routieres (1993).
[18] AASHTO R 28 Standard practice for accelerated aging of asphalt binder using a Pressurized Aging Vessel, American Association of State Highway and Transportation Officials, Washington, D.C, 2012.
[19] F. Migliori, J.-F. Corté, Comparative study of RTFOT and PAV aging simulation laboratory tests, Transportation Research Record: Journal of the Transportation Research Board (1638) (1998) 56-63.
[20] S.-C. Huang, M. Tia, E. Ruth Byron, Laboratory Aging Methods for Simulation of Field Aging of Asphalts, Journal of Materials in Civil Engineering 8(3) (1996) 147-152.
[21] M. Wong, F. Peng, B. Zou, W. Shi, G.J.I.j.o.e.r. Wilson, p. health, Spatially analyzing the inequity of the Hong Kong urban heat island by socio-demographic characteristics, 13(3) (2016) 317.
[22] ASTM D2172, Standard Test Methods for Quantitative Extraction of Asphalt Binder from Asphalt Mixtures, ASTM International, West Conshohocken, PA, 2011.
[23] ASTM D5404, Standard Practice for Recovery of Asphalt from Solution Using the Rotary Evaporator, ASTM International, West Conshohocken,PA, 2012.
[24] J. Lamontagne, P. Dumas, V. Mouillet, J. Kister, Comparison by Fourier transform infrared (FTIR) spectroscopy of different ageing techniques: application to road bitumens, Fuel 80(4) (2001) 483-488.
[25] Q. Qin, J.F. Schabron, R.B. Boysen, M.J. Farrar, Field aging effect on chemistry and rheology of asphalt binders and rheological predictions for field aging, Fuel 121(Supplement C) (2014) 86-94.
[26] H. Yao, Z. You, L. Li, S.W. Goh, C.H. Lee, Y.K. Yap, X. Shi, Rheological properties and chemical analysis of nanoclay and carbon microfiber modified asphalt with Fourier transform infrared spectroscopy, Construction and Building Materials 38(Supplement C) (2013) 327-337.
[27] Y. Zhang, Z. Leng, Quantification of bituminous mortar ageing and its application in ravelling evaluation of porous asphalt wearing courses, Materials & Design 119(Supplement C) (2017) 1-11.

[28] X. Yang, J. Mills-Beale, Z. You, Chemical characterization and oxidative aging of bio-asphalt and its compatibility with petroleum asphalt, Journal of Cleaner Production 142(Part 4) (2017) 1837-1847.
[29] C. Yan, W. Huang, Q. Lv, Study on bond properties between RAP aggregates and virgin asphalt using Binder Bond Strength test and Fourier Transform Infrared spectroscopy, Construction and Building Materials 124(Supplement C) (2016) 1-10.
[30] H. Yao, Q. Dai, Z. You, Fourier Transform Infrared Spectroscopy characterization of aging-related properties of original and nano-modified asphalt binders, Construction and Building Materials 101(Part 1) (2015) 1078-1087.
[31] A. Dony, L. Zyian, I. Drouadaine, S. Pouget, S. Faucon-Dumont, D. Simard, V. Mouillet, T. Gabet, L. Boulange, A. Nicolai, MURE National Project: FTIR spectroscopy study to assess ageing of asphalt mixtures, Proceedings of the E&E congress, 2016.
[32] Z. Leng, A. Sreeram, R.K. Padhan, Z. Tan, Value-added application of waste PET based additives in bituminous mixtures containing high percentage of reclaimed asphalt pavement (RAP), Journal of cleaner production 196 (2018) 615-625.
[33] X. Luo, F. Gu, R.L. Lytton, Prediction of field aging gradient in asphalt pavements, Transportation Research Record 2507(1) (2015) 19-28.
[34] E.L. Omairey, Y. Zhang, S. Al-Malaika, H. Sheena, F. Gu, Impact of anti-ageing compounds on oxidation ageing kinetics of bitumen by infrared spectroscopy analysis, Construction and Building Materials 223 (2019) 755-764.
[35] AASHTO 240 Standard Method of Test for Effect of Heat and Air on a Moving Film of Asphalt Binder (Rolling Thin-Film Oven Test), American Association of State Highway Transportation Officials, Washington, D.C, 2013.
[36] ASTM D36 Standard Test Method for Softening Point of Bitumen (Ring-and-Ball Apparatus), ASTM International, West Conshohocken, PA, 2014.
[37] ASTM D5 Standard Test Method for Penetration of Bituminous Materials, ASTM International, West Conshohocken, PA, 2013.
[38] AASHTO M320 Performance-Graded Asphalt Binder, American Association of State Highway and Transportation Officials, Washington, D.C, 2016.
[39] AASHTO T315-12, Determining The Rheological Properties Of Asphalt Binder Using A Dynamic Shear Rheometer (DSR), American Association of State Highway and Transportation Officials, Washington, D.C, 2013, p. 32.
[40] H. Zhu, L. Sun, J. Yang, Z. Chen, W. Gu, Developing Master Curves and Predicting Dynamic Modulus of Polymer-Modified Asphalt Mixtures, Journal of Materials in Civil Engineering 23(2) (2011) 131-137.
[41] Y. Zhao, J. Tang, H. Liu, Construction of triaxial dynamic modulus master curve for asphalt mixtures, Construction and Building Materials 37 (2012) 21-26.
[42] A. Booshehrian, S. Mogawer Walaa, R. Bonaquist, How to Construct an Asphalt Binder Master Curve and Assess the Degree of Blending between RAP and Virgin Binders, Journal of Materials in Civil Engineering 25(12) (2013) 1813-1821.
[43] M. Ling, X. Luo, F. Gu, R.L. Lytton, Time-temperature-aging-depth shift functions for dynamic modulus master curves of asphalt mixtures, Construction and Building Materials 157 (2017) 943-951.
[44] M.F. Woldekidan, M. Huurman, A.C. Pronk, A modified HS model: Numerical applications in modeling the response of bituminous materials, Finite Elements in Analysis and Design 53 (2012) 37-47.
[45] A.C. Pronk, The Huet-Sayegh Model; A simple and excellent rheological model for master curves of asphaltic mixes, Asphalt Concrete Simulation, Modeling, and Experimental Characterization. R. Lytton Symposium on Mechanics of Flexible PavementsAmerican Society of Civil Engineers, 2006.
[46] D.A. Anderson, D.W. Christensen, H. Bahia, Physical properties of asphalt cement and the development of performance-related specifications, Journal of the Association of Asphalt Paving Technologists 60 (1991).
[47] D.W. Christensen, D.A. Anderson, Interpretation of dynamic mechanical test data for paving grade asphalt cements (with discussion), Journal of the Association of Asphalt Paving Technologists 61 (1992).

509 [48] W. Van den Bergh, The effect of ageing on the fatigue and healing properties of bituminous mortars,
510 (2011).
511 [49] D.O. Larsen, J.L. Alessandrini, A. Bosch, M.S. Cortizo, Micro-structural and rheological
512 characteristics of SBS-asphalt blends during their manufacturing, Construction and Building Materials
513 23(8) (2009) 2769-2774.
514 [50] Y.R. Kim, S. Underwood, Long-term aging of asphalt mixtures for performance testing and
515 prediction (2018).

516
517